



**University of
Zurich**^{UZH}

**Zurich Open Repository and
Archive**

University of Zurich
University Library
Strickhofstrasse 39
CH-8057 Zurich
www.zora.uzh.ch

Year: 2014

The MutS complex is a modulator of p53-driven tumorigenesis through its functions in both DNA double-strand break repair and mismatch repair

van Oers, J M M ; Edwards, Y ; Chahwan, R ; Zhang, W ; Smith, C ; Pechuan, X ; Schaetzlein, S ; Jin, B ; Wang, Y ; Bergman, A ; Scharff, M D ; Edelmann, W

Abstract: Loss of the DNA mismatch repair (MMR) protein MSH3 leads to the development of a variety of tumors in mice without significantly affecting survival rates, suggesting a modulating role for the MutS (MSH2-MSH3) complex in late-onset tumorigenesis. To better study the role of MSH3 in tumor progression, we crossed Msh3(-/-) mice onto a tumor predisposing p53-deficient background. Survival of Msh3/p53 mice was not reduced compared with p53 single mutant mice; however, the tumor spectrum changed significantly from lymphoma to sarcoma, indicating MSH3 as a potent modulator of p53-driven tumorigenesis. Interestingly, Msh3(-/-) mouse embryonic fibroblasts displayed increased chromatid breaks and persistence of H2AX foci following ionizing radiation, indicating a defect in DNA double-strand break repair (DSBR). Msh3/p53 tumors showed increased loss of heterozygosity, elevated genome-wide copy-number variation and a moderate microsatellite instability phenotype compared with Msh2/p53 tumors, revealing that MSH2-MSH3 suppresses tumorigenesis by maintaining chromosomal stability. Our results show that the MSH2-MSH3 complex is important for the suppression of late-onset tumors due to its roles in DNA DSBR as well as in DNA MMR. Further, they demonstrate that MSH2-MSH3 suppresses chromosomal instability and modulates the tumor spectrum in p53-deficient tumorigenesis and possibly has a role in other chromosomally unstable tumors as well.

DOI: <https://doi.org/10.1038/onc.2013.365>

Posted at the Zurich Open Repository and Archive, University of Zurich

ZORA URL: <https://doi.org/10.5167/uzh-168153>

Journal Article

Published Version

Originally published at:

van Oers, J M M; Edwards, Y; Chahwan, R; Zhang, W; Smith, C; Pechuan, X; Schaetzlein, S; Jin, B; Wang, Y; Bergman, A; Scharff, M D; Edelmann, W (2014). The MutS complex is a modulator of p53-driven tumorigenesis through its functions in both DNA double-strand break repair and mismatch repair. *Oncogene*, 33(30):3939-3946.

DOI: <https://doi.org/10.1038/onc.2013.365>

ORIGINAL ARTICLE

The MutS β complex is a modulator of p53-driven tumorigenesis through its functions in both DNA double-strand break repair and mismatch repair

JMM van Oers^{1,4}, Y Edwards^{1,4}, R Chahwan¹, W Zhang², C Smith³, X Pechuan³, S Schaetzlein¹, B Jin¹, Y Wang¹, A Bergman³, MD Scharff¹ and W Edelmann¹

Loss of the DNA mismatch repair (MMR) protein MSH3 leads to the development of a variety of tumors in mice without significantly affecting survival rates, suggesting a modulating role for the MutS β (MSH2-MSH3) complex in late-onset tumorigenesis. To better study the role of MSH3 in tumor progression, we crossed *Msh3*^{-/-} mice onto a tumor predisposing *p53*-deficient background. Survival of *Msh3/p53* mice was not reduced compared with *p53* single mutant mice; however, the tumor spectrum changed significantly from lymphoma to sarcoma, indicating MSH3 as a potent modulator of p53-driven tumorigenesis. Interestingly, *Msh3*^{-/-} mouse embryonic fibroblasts displayed increased chromatid breaks and persistence of γ H2AX foci following ionizing radiation, indicating a defect in DNA double-strand break repair (DSBR). *Msh3/p53* tumors showed increased loss of heterozygosity, elevated genome-wide copy-number variation and a moderate microsatellite instability phenotype compared with *Msh2/p53* tumors, revealing that MSH2-MSH3 suppresses tumorigenesis by maintaining chromosomal stability. Our results show that the MSH2-MSH3 complex is important for the suppression of late-onset tumors due to its roles in DNA DSBR as well as in DNA MMR. Further, they demonstrate that MSH2-MSH3 suppresses chromosomal instability and modulates the tumor spectrum in *p53*-deficient tumorigenesis and possibly has a role in other chromosomally unstable tumors as well.

Oncogene (2014) 33, 3939–3946; doi:10.1038/onc.2013.365; published online 9 September 2013

Keywords: DNA mismatch repair; MSH2-MSH3; DNA double-strand break repair; chromosomal instability; p53; sarcomagenesis

INTRODUCTION

DNA mismatch repair (MMR) complexes function primarily in the detection and repair of mismatched bases that result from erroneous replication. Two heterodimeric MutS homolog (MSH) complexes, consisting of either MSH2-MSH6 (MutS α) or MSH2-MSH3 (MutS β), are responsible for the recognition of these mismatched bases. MSH2-MSH6 binds to single base–base mismatches and small insertions/deletions, whereas MSH2-MSH3 has a higher affinity for ≥ 2 base insertions/deletions.^{1,2} Germline mutations in *MSH2* and *MSH6* but not *MSH3* are responsible for hereditary non-polyposis colorectal cancer/Lynch syndrome (HNPCC/LS); however, an (A)8 tract in the coding region of *MSH3* was found to be frequently affected by frameshift mutations in MMR-deficient colorectal tumors, resulting in the loss of MSH3 protein expression.³ In addition to its role in MMR, yeast studies revealed that during non-conservative homologous recombination, the MSH2-MSH3 complex is required to remove nonhomologous DNA ends during both the initiation of gene conversion and the resolution of single-strand annealing (SSA) intermediates that are initiated by a double-strand break (DSB).^{4,5} SSA is a subset of the homologous recombination pathway for repairing spontaneous and induced DSBs that arise between repeated sequences occurring in *cis*. MSH2 and MSH3 recognize and stabilize the nonhomologous 3' tails at the junction of double-stranded and single-stranded DNA to aid in either the recruitment or cleavage activity of Rad1-Rad10.⁶ Although the mechanistic

contribution of MSH3 in MMR and double-strand break repair (DSBR) was thought to be overlapping, recent studies have shown that these two MSH3 activities are molecularly distinct.⁷ MSH2-MSH3 is also involved in triplet repeat (CAG·CTG) expansion diseases such as Huntington and myotonic dystrophy, and it has been shown in several mouse models that MSH2 and MSH3 are absolutely required to generate these expansions.^{8–12}

Previous observations showed that inactivation of *Msh3* in mice leads to a moderate defect in the repair of insertion/deletion but not base–base mismatches,¹³ which might explain the absence of *MSH3* mutations in HNPCC/LS families. Among other tumors, *Msh3*^{-/-} mice developed gastrointestinal tumors late in life, which corresponds with loss of MSH3 expression in late-onset sporadic colorectal cancer in humans.¹⁴ In human cancers, loss of MSH3 is associated with an (microsatellite instability) MSI-low (MSI-L) phenotype at dinucleotide repeats and elevated microsatellite alterations at selected tetranucleotide repeats (EMAST).^{15,16} Loss or silencing of *MSH3* also frequently occurs in a variety of other cancers, including non-small cell lung,¹⁷ ovarian, bladder,¹⁸ and breast¹⁹ cancer. *MSH3* polymorphisms were found to be associated with sporadic colorectal,^{14,20,21} prostate,²² and lung²³ cancer. These findings correlate with a recent report that unlike MutS α , the MutS β complex is abundant in the majority of mouse tissues.²⁴ Taken together, these studies indicate that MSH2-MSH3 might be important for tumor suppression in multiple tissues and especially in cases of late-onset tumorigenesis.

¹Department of Cell Biology, Albert Einstein College of Medicine, Bronx, NY, USA; ²Department of Medicine, Mount Sinai School of Medicine, New York, NY, USA and ³Department of Systems and Computational Biology, Albert Einstein College of Medicine, Bronx, NY, USA. Correspondence: Dr W Edelmann, Department of Cell Biology, Albert Einstein College of Medicine, 1301 Morris Park Avenue, Bronx, NY 10461, USA.

E-mail: winfried.edelmann@einstein.yu.edu

⁴These authors contributed equally to this work.

Received 23 May 2013; revised 19 July 2013; accepted 30 July 2013; published online 9 September 2013

Previous studies in mice showed that loss of *Msh2* is sufficient to initiate and significantly accelerate tumorigenesis, especially in *p53*-deficient mice, and that tumorigenesis is associated with an MSI-high (MSI-H) phenotype.²⁵ The MSH2-MSH6 complex is essential for the repair of base/base mismatches, and loss of either MSH2 or MSH6 therefore results in generation of a severe mutator phenotype and early-onset cancers. In contrast, the absence of *MSH3* mutations in early-onset HNPCC/LS tumors and the late-onset tumor phenotype in *Msh3*^{-/-} mice indicate that MSH3 is likely not involved in tumor initiation. To determine a possible role for MSH2-MSH3 in tumor progression, we crossed *Msh3*-null mice onto the tumor predisposing *p53*-null background to create cohorts of both *Msh3*^{-/-}*p53*^{-/-} and *Msh3*^{-/-}*p53*^{+/-} mice, compared their cancer predisposition phenotype with MMR-deficient *Msh2/p53*-mutant mice and analyzed the underlying molecular mechanisms. Although the effects of both *Msh2*- and *Msh3*-deficiency manifest from the earliest stages of life, tumor onset in *Msh3*^{-/-}*p53*^{-/-} mice occurred later in life in contrast to the early-onset tumorigenesis in *Msh2*^{-/-}*p53*^{-/-} mice. We found that because of its role in DSBR in addition to MMR, loss of *Msh3* alters the tumor spectrum in *p53*-mutant mice by modulating the characteristics of the chromosomal instability (CIN) phenotype, resulting in elevated sarcomagenesis. We conclude that germline mutations in *Msh3* can

cause late-onset tumorigenesis with various genomic signatures and modulate the tumor spectrum on cancer predisposing backgrounds.

RESULTS

Altered cancer phenotype and elevated sarcomagenesis in *Msh3/p53*-mutant mice

To accelerate tumorigenesis in *Msh3*-null mice and study tumor progression, we intercrossed *Msh3*^{+/-} and *p53*^{+/-} knockout mice and generated two cohorts of mutant mice carrying homozygous mutations in *Msh3* and either homozygous (*Msh3*^{-/-}*p53*^{-/-}) or heterozygous (*Msh3*^{-/-}*p53*^{+/-}) mutations in *p53*. To compare loss of *Msh3* with the classic MMR phenotype, additional *Msh2*^{-/-}*p53*^{-/-} and *Msh2*^{-/-}*p53*^{+/-} cohorts were generated by intercrossing *Msh2*^{+/-} and *p53*^{+/-} mice.

Msh3^{-/-}*p53*^{-/-} double-mutant mice showed reduced survival (median survival time 5 months, Figure 1a) when compared with *Msh3*^{-/-} alone (22 months),¹³ but not when compared with *p53*^{-/-} single-mutant mice (*P*=0.31, Figure 1a). *Msh3*^{-/-}*p53*^{+/-} and *p53*^{+/-} mice also showed similar survival rates (*P*=0.11), suggesting that loss of *Msh3* does not contribute to the initiation or acceleration of tumorigenesis. In contrast, *Msh2*^{-/-}*p53*^{-/-} and *Msh2*^{-/-}*p53*^{+/-} mice showed

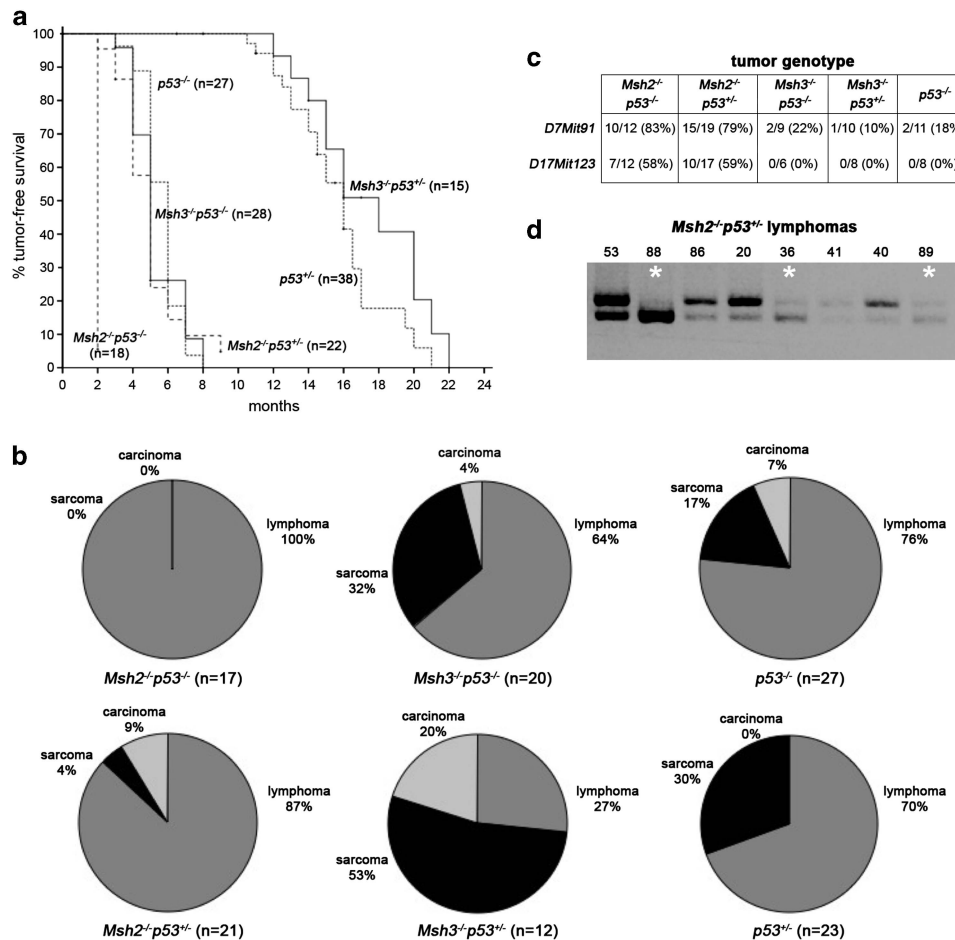


Figure 1. Loss of *Msh3* modifies tumor phenotype of *p53*-null mice. (a) Tumor-free survival was significantly different for *Msh2*^{-/-}*p53*^{-/-} and *p53*^{-/-} mice (*P*<0.001) and for *Msh2*^{-/-}*p53*^{+/-} and *p53*^{+/-} mice (*P*<0.001). In contrast, survival was similar for *Msh3*^{-/-}*p53*^{-/-} and *p53*^{-/-} mice (*P*=0.31) and for *Msh3*^{-/-}*p53*^{+/-} and *p53*^{+/-} mice (*P*=0.11). Dashed lines, *Msh2/p53* genotypes; solid lines, *Msh3/p53* genotypes; dotted lines, single *p53* genotypes. (b) Tumor type and incidence in mice with different *Msh2*, *Msh3* and *p53* genotypes. The percentage of sarcomas is increased in *Msh3*^{-/-}*p53*^{-/-} and *Msh3*^{-/-}*p53*^{+/-} mice compared with *p53*^{-/-} and *p53*^{+/-} mice, respectively (*P*=0.04). Also, the carcinoma phenotype includes a small number of small intestinal tumors (*Msh3*^{-/-}*p53*^{-/-}, 1; *Msh3*^{-/-}*p53*^{+/-}, 2). (c) Microsatellite instability (MSI) analysis of tumors at the dinucleotide loci D7Mit91 and D17Mit123, determined by the number of unstable alleles divided by the total number of alleles scored. (d) Loss of heterozygosity (LOH) of the wild-type *p53* allele (*) was demonstrated in *Msh2*^{-/-}*p53*^{+/-} or *Msh3*^{-/-}*p53*^{+/-} tumor samples using PCR (see also Table 1). Upper band, wild-type allele (540 bp); lower band, *p53*-null allele (480 bp).

significantly reduced survival compared with *p53*^{-/-} (2 vs 6 months, *P*<0.001) and *p53*^{+/-} (5 vs 16 months, *P*<0.001) mice, respectively, confirming the strong tumorigenic MMR-deficient phenotype that has previously been described for *Msh2*^{-/-},²⁶⁻²⁸ *Msh2*^{-/-}*p53*^{-/-}²⁵ and *Msh2*^{-/-}*p53*^{+/-}²⁹ mice.

The tumor spectrum of *p53*^{-/-} mice is dominated by lymphomas, but also includes sarcomas and carcinomas.³⁰ Surprisingly, loss of *Msh3* induced a significant shift in the distribution of the various tumor types in *p53*-mutant mice: twice as many sarcomas were found in *Msh3*^{-/-}*p53*^{-/-} (32 vs 17%, *P*=0.04) and *Msh3*^{-/-}*p53*^{+/-} mice (53 vs 30%, *P*=0.04, Figure 1b) compared with tumors from *p53*^{-/-} and *p53*^{+/-} mice, respectively. In contrast, nearly 100% of MMR-deficient *Msh2*^{-/-}*p53*^{-/-} and *Msh2*^{-/-}*p53*^{+/-} mice succumbed to thymic lymphoma. Only a small number of *Msh3/p53* mice developed gastrointestinal tumors. When tumors were analyzed for their MSI phenotype, which is the hallmark of MMR deficiency, we found that most tumors from *Msh2*^{-/-}*p53*^{-/-} or *Msh2*^{-/-}*p53*^{+/-} mice showed MSI at the D7Mit91 and D17Mit123 dinucleotide repeats, compared with few tumors with MSI from *Msh3*^{-/-}*p53*-mutant mice (Figure 1c). Interestingly, none of the sarcoma samples included in the analysis (0/12) showed MSI. The MSI-L tumor phenotype indicates that defective MMR of insertion/deletion mutations is not a main mechanism in *Msh3*^{-/-}*p53*-driven tumorigenesis.

LOH but not somatic mutation leads to loss of the wild-type *p53* allele in *Msh3*^{-/-}*p53*^{+/-} tumors
During tumorigenesis, MMR deficiency leads to the accumulation of somatic mutations in tumor suppressor genes and oncogenes.

On the other hand, tumors with CIN usually display loss of heterozygosity (LOH) of tumor suppressor genes, which is often associated with defective DSB repair pathways.³¹ As loss of the tumor suppressor *p53* is a critical event in tumorigenesis, we studied the genetic mechanisms by which the remaining *p53* wild-type allele was lost in *Msh3*^{-/-}*p53*^{+/-} and *Msh2*^{-/-}*p53*^{+/-} tumors. Consistent with the MMR-deficient phenotype, the majority of *Msh2*^{-/-}*p53*^{+/-} tumors (63%, 12/19, Table 1) showed mutation of *p53*. All *p53* exons were sequenced, and mutations were found in exons 4, 5, 7, 8, 9 and 11 of *Msh2*^{-/-}*p53*^{+/-} tumors. In contrast, no *p53* mutations were detected in the *Msh3*^{-/-}*p53*^{+/-} tumors (0/8); however, LOH at the wild-type *p53* allele occurred in almost all of the tumors (86%, 6/7) (Figure 1d and Table 1), suggesting a possible role for MSH3 in CIN. LOH of the wild-type *p53* allele was also found in some *Msh2*^{-/-}*p53*^{+/-} tumors (3/19, 16%), possibly reflecting loss of MSH2-MSH3 function in DSB repair.

Msh3-deficient MEFs are defective in DSB repair

In yeast, MSH2-MSH3 is involved in the processing of SSA recombination intermediates during certain forms of homologous recombination,⁵ and loss of this function might result in defective DSB repair and contribute to the LOH phenotype in the tumors of *Msh2*^{-/-}*p53*^{+/-} and *Msh3*^{-/-}*p53*^{+/-} mice. To investigate whether mouse MSH3 functions as part of the MSH2-MSH3 complex in the repair of DNA breaks, we first analyzed metaphases of untreated primary mouse embryonic fibroblast (MEF) cell lines. *Msh3*^{-/-} and *Msh2*^{-/-} MEFs both showed a significant increase in chromatid breaks (Figures 2a and b), further indicating a defective DSB repair response. As the number of breaks in *Msh6*^{-/-} cells was not significantly different from that in wild-type cells

Table 1. <i>p53</i> mutation and LOH in <i>p53</i> ^{+/-} tumors							
Tumor sample	Exon 4	Exon 5	Exon 7	Exon 8	Exon 9	Exon 11.1	LOH
<i>Msh2</i> ^{-/-} <i>p53</i> ^{+/-}							
29						del (A) ₇	
47						del (A) ₇	
90							
66l	ins (T) ₆						
73	Q112STOP						
65							null
49							
48							
66ll	ND			del (A) ₅	del (C) ₅	ND	
63	ND			del (C) ₅	ND	ND	
53	ND		del (G) ₆		ND	ND	
88	ND	Q141STOP			ND	ND	wt
86	ND			del (A) ₅	ND	ND	
20							
36							wt
41	ND			del (C) ₅	ND	ND	
40	ND		del (G) ₆		ND	ND	
89							wt
14							
<i>Msh3</i> ^{-/-} <i>p53</i> ^{+/-}							
43	ND				ND	ND	wt
42	ND				ND	ND	wt
45	ND				ND	ND	wt
56	ND				ND	ND	ND
66	ND				ND	ND	wt
54	ND	ND			ND	ND	ND
36							
64	ND	ND			ND	ND	ND
15	ND	ND	ND	ND	ND	ND	wt
19	ND	ND	ND	ND	ND	ND	wt

Abbreviation: ND, not determined.

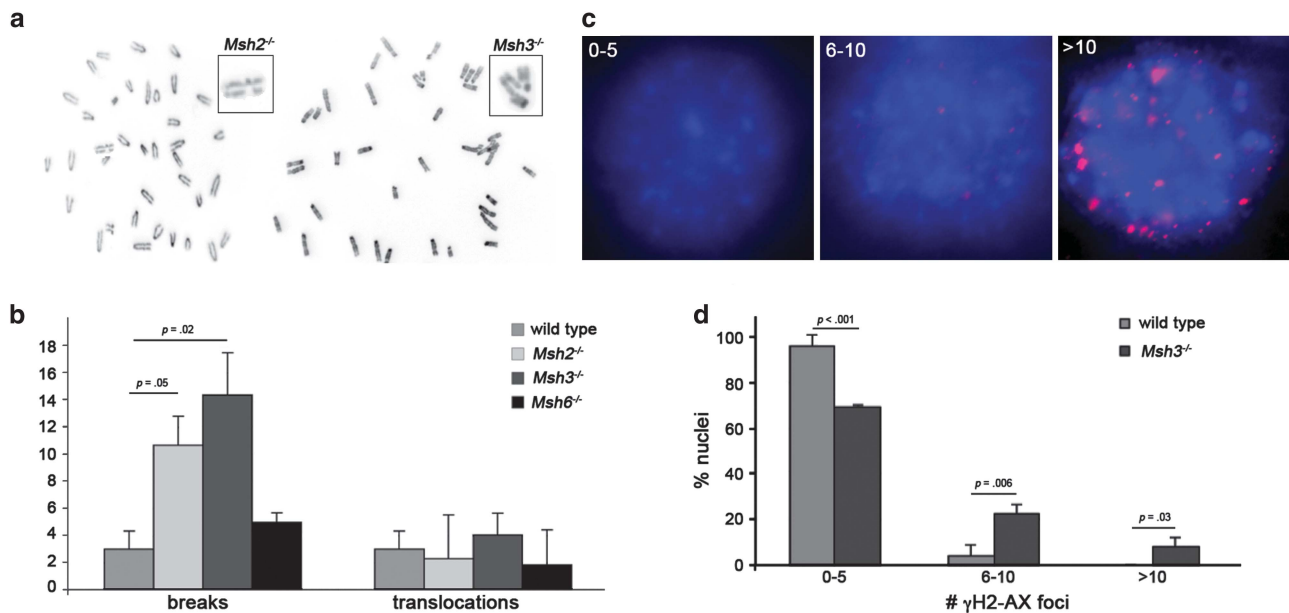


Figure 2. Loss of *Msh3* induces a double-strand break repair defect. **(a)** Metaphase spreads from *Msh2*^{-/-} (left) and *Msh3*^{-/-} (right) mouse embryonic fibroblasts (MEFs). Examples of chromatid breaks are magnified in insets. **(b)** Chromosomal aberrations were analyzed for >100 metaphase nuclei per genotype in MEF cell lines. Average numbers of chromatid breaks and translocations are shown. **(c)** Three categories of γH2AX foci accumulation were defined after staining with DAPI (blue) and anti-γH2AX antibody (red): 0–5, 6–10 and >10 foci per nucleus. **(d)** Deficient double-strand break repair was defined by accumulation of γH2AX foci in *Msh3*^{-/-} and wild-type MEFs 6 h after irradiation with 1 Gy.

($P = 0.21$), loss of DSB repair appears to be specifically due to the loss of MSH2-MSH3 complex function. Notably, all genotypes showed similar numbers of translocations.

To further analyze the observed DSB repair defect, *Msh3*^{-/-} cells were subjected to a low dose of ionizing radiation (1 Gy), and efficient resolution of DSBs was subsequently evaluated by counting γH2AX foci in the cell nuclei (Figure 2c). We did not observe a difference in the number of γH2AX foci 1 h after irradiation (Supplementary Figure S1), which suggests that both wild-type and *Msh3*^{-/-} MEFs had a comparable accumulation of DSBs at early time points and that γH2AX signaling is intact in *Msh3*^{-/-} cells. However, 2 h after irradiation, the majority of wild-type cells (95%) showed background levels of 0–10 γH2AX foci per nucleus in contrast to only 45% of *Msh3*^{-/-} cells (Supplementary Figure S1). Even 6 h post irradiation, only 70% of *Msh3*^{-/-} cells were able to adequately resolve DSBs ($P < 0.001$, Figure 2d), and an increase of more than 10 γH2AX foci per nucleus could be seen in the remaining 30% of nuclei. Taken together, these data demonstrate a moderate DSB repair defect in *Msh3*-deficient cells that is revealed by a delay in resolving DSBs.

Msh3 deletion is associated with CIN in p53-deficient tumors

To examine whether loss of MSH3 does lead to CIN during tumorigenesis, we used spectral karyotyping (SKY) to determine whether lymphomas of *Msh3*-deficient mice displayed any gross chromosomal abnormalities. In contrast to *Msh2*^{-/-}*p53*^{-/-} tumor cells, which showed close to normal ploidy (40 chromosomes/cell, Table 2), *Msh3*^{-/-}*p53*^{-/-} tumor cell karyotypes showed increased CIN characterized by significantly increased aneuploidy (55 chromosomes/cell, $P < 0.001$), translocations, deletions, duplications and breaks (Figure 3). No specific recurring chromosomal aberrations were found, indicating that loss of MSH3 induces general CIN. However, the type of chromosomal changes between genotypes tended to be different: *Msh3*^{-/-}*p53*^{-/-} and *Msh2*^{-/-}*p53*^{-/-} tumor cells showed about two times more translocations compared with *p53*^{-/-} cells (1.2 and

Table 2. Chromosomal aberrations from SKY analysis

Tumor sample	No of Cells	Average no aberrations per cell (± 95% CI)		
		Chromosomes	Translocations	Deletions/duplications
<i>Msh3</i> ^{-/-} <i>p53</i> ^{-/-}	23	55 ^a (51–83)	1.2 (0.4–1.9)	1.0 (0.4–1.5)
<i>Msh2</i> ^{-/-} <i>p53</i> ^{-/-}	26	40 (39–41)	0.9 (0.5–1.3)	0.7 (0.2–1.2)
<i>p53</i> ^{-/-}	17	51 (51–54)	0.5 (0.1–0.8)	1.2 (0.4–1.9)

Abbreviation: CI, confidence interval. ^aBoth *Msh3*^{-/-}*p53*^{-/-} ($P < 0.001$) and *p53*^{-/-} ($P = 0.001$) tumors have significantly more chromosomes per cell compared with *Msh2*^{-/-}*p53*^{-/-} tumor cells.

0.9 vs 0.5 per cell, Table 2), suggesting that the DSB repair defect associated with loss of the MSH2-MSH3 complex that was observed earlier contributes to this type of chromosomal rearrangement. In contrast, a trend toward slightly higher numbers of deletions and duplications was observed in *Msh3*^{-/-}*p53*^{-/-} and *p53*^{-/-} cells compared with *Msh2*^{-/-}*p53*^{-/-} cells, reflecting the aneuploidy phenotype that is associated with the *p53*^{-/-} tumor background.

To study the increase in CIN in *Msh3/p53* tumors in more detail, we used the lymphoma samples that were used for SKY analysis in array comparative genomic hybridization (aCGH) to analyze genome-wide copy-number variation (CNV). As loss of *Msh3* induces sarcomagenesis, we also analyzed two groups of *Msh3*^{-/-}*p53*^{+/+} and *p53*^{-/-} sarcomas (Supplementary Figure S2). Again, no increase in CNV was found to recur between samples at specific genomic regions, indicating general CIN. Compared with *Msh2*^{-/-}*p53*^{-/-} lymphoma samples, in which CNV was uncommon, this type of instability was significantly increased in *Msh3*^{-/-}*p53*^{-/-} and *p53*^{-/-} lymphomas (Figure 4).



Figure 3. MSH3 is involved in maintaining chromosomal stability. Examples of spectral karyotypes from lymphoma cells are shown for each genotype, indicating a close to normal karyotype and t(1,8) for *Msh2*^{-/-} *p53*^{-/-}, increased aneuploidy, del1 and t(1,7) for *Msh3*^{-/-} *p53*^{-/-}, and increased aneuploidy, 2del1 and del6 for *p53*^{-/-}. Red boxes indicate translocations and deletions.

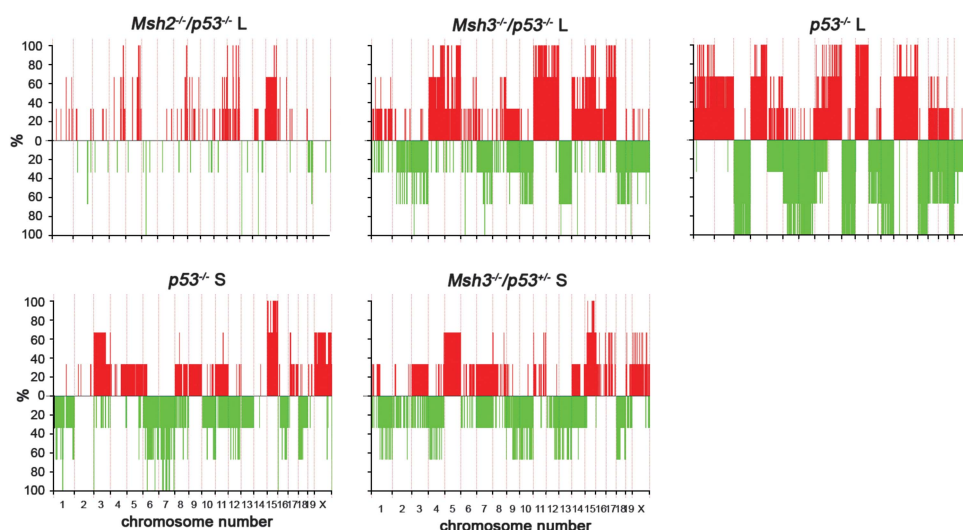


Figure 4. Loss of *Msh3* is associated with a high level of CNV. Chromosome copy-number changes were analyzed as described before.⁴² To account for tumor heterogeneity, large segments with low-level copy-number changes were considered as small segments with high-level changes, and no arbitrary log2 ratio was used. %, percentage of samples that showed gain (red) or loss (green). L, lymphoma; S, sarcoma.

Log2 ratio distributions of gains and losses (Supplementary Figure S3) and subsequent cluster analysis (Supplementary Figure S4) revealed that both *p53*^{-/-} and *Msh3*^{-/-} *p53*^{-/-} lymphomas showed a significant increase in CNV (cluster 1) compared with *Msh2*^{-/-} *p53*^{-/-} tumors (cluster 3). *Msh3*^{-/-} *p53*^{-/-} and *p53*^{-/-} lymphoma samples clustered together (cluster 1) that indicates the overall distribution of CNVs throughout the genome in *Msh3*^{-/-} *p53*^{-/-} tumors was similar to that of *p53*^{-/-} tumors and that loss of MSH3 does not induce a specific pattern of CNV distribution. Interestingly, the *Msh3/p53* and *p53* sarcoma samples (cluster 2) only showed a moderate increase in CNV compared with *Msh3/p53* and *p53* lymphoma samples. However, the CNV phenotype in *Msh3/p53* sarcomas was significantly more severe than that found in *Msh2/p53* lymphoma samples. Taken together, these results confirm that

loss of MSH3, but not MSH2, is associated with an increase in overall CIN in tumor genomes and that the amount of CIN depends on the underlying predisposing genetic background and the tissue-specific context.

DISCUSSION

The MMR proteins MSH2, MSH6, MLH1 and PMS2 all have a major and well-described role in MMR, and mutations in these genes have been found in patients with HNPCC/LS. Until now, no mutations have been found in the other MMR proteins MSH3, MLH3 and EXO1 that could directly link them to the development of familial colorectal cancer. Although intestinal tumors developed in *Msh3*¹³ and *Mlh3*³² knockout mice late in life, these proteins appear to have a less pronounced role in MMR and tumor

suppression. However, they have been implicated in other processes aside from MMR: apart from their roles in class switch recombination and somatic hypermutation,^{33–36} MLH3 is essential for processing DSBs at crossovers during meiosis,³⁷ and EXO1 has been identified as a key mediator of DNA end resection during DSBR.³⁸ Surprisingly, it has recently been found that MSH3 protein expression is higher in the majority of murine tissues when compared with MSH6, suggesting important and specific roles for MSH2-MSH3 in DNA repair and genomic instability.²⁴ The similar phenotype of late-onset tumors with mild MSI that appeared in *Msh3*^{−/−} and *Exo1*^{−/−} mice led us to hypothesize a role for MSH3 in tumor suppression via DSBR and maintenance of chromosomal stability. In this study, we showed that, in mice, loss of *Msh3* leads to accumulation of unrepaired DSBs and to a shift in tumor spectrum with increased CIN on a *p53*-driven tumor predisposing background.

As described before,²⁵ mice with combined *Msh2* and *p53* ablation show independent segregation of the MSI phenotype compared with *p53*^{−/−} alone, which suggests that loss of *Msh2* is dominant over the *p53*^{−/−} phenotype. Furthermore, their synergism in tumorigenesis suggests that they are not genetically epistatic. In contrast, *Msh3*^{−/−}*p53*^{−/−} mice show features that are more similar to the *p53*^{−/−} phenotype. The lack of synergism in tumorigenesis and the shift in tumor spectrum toward sarcomagenesis suggest that MSH3 might not be involved in tumor initiation but rather in tumor progression by modulating the *p53*-deficient phenotype. Interestingly, loss of *p53* did not accelerate gastrointestinal tumorigenesis of *Msh3*^{−/−} mice, as we only detected a small number of gastrointestinal carcinomas in *Msh3/p53*-mutant mice (Figure 1b). As loss of MSH3 is associated with a variety of human cancer types, its effects might be evident on other predisposing backgrounds, implicating MSH3 as a general modulator of cancer phenotypes. The contribution of *Msh3* deletion to tumorigenesis, however, depends on the genetic context and subsequent mechanism of tumorigenesis in different tissues, as *Msh3*^{−/−}*Apc*^{1638N} mice did not show a different tumor onset or phenotype compared with *Apc*^{1638N} mice.³⁹

Because of the strong aneuploidy phenotype caused by loss of *p53*,^{40,41} it was not immediately clear whether loss of *Msh3* contributed to the increase in CIN in *Msh3*^{−/−}*p53*^{−/−} tumors. However, although there was only a limited number of tumor samples available for SKY analysis, we observed differences between tumors with combined *Msh3/p53* deficiency and single *p53* deficiency with a trend toward an increase in the average number of translocations per cell for *Msh3*^{−/−}*p53*^{−/−} tumors compared with *p53*^{−/−} alone, indicating defective DSBR caused by loss of the MSH2-MSH3 complex in these tumors. This defect in DSBR was also visible when we counted chromosomal aberrations in metaphase spreads, showing a significant increase in chromatid breaks in *Msh3*^{−/−} and *Msh2*^{−/−} MEFs. Interestingly, here the number of translocations was not significantly different between wild-type, *Msh3*^{−/−} and *Msh2*^{−/−} MEFs, which might be due to technical difficulties with scoring translocations in regular metaphase spreads. Alternatively, these data suggest that loss of MSH2-MSH3-dependent DSBR results in an increase in the number of translocations during the clonal outgrowth of *p53*-deficient tumors and contributes to *p53*-driven tumorigenesis. The amount of CIN represented by CNV, however, is significantly increased in *Msh3*^{−/−}*p53*^{+/−} tumors (Figure 4 and Supplementary Figure S2) compared with the CNV phenotype in *p53*^{+/−} tumors from our previous study,⁴² which indicates that loss of *Msh3* is contributing to the CIN phenotype in *Msh3*^{−/−}*p53*^{+/−} tumors.

Our observations indicate a dual function for the MutSβ complex in genome maintenance and tumor suppression (Figure 5). *Msh2*-deficient mice display a strong MMR defect with accumulation of mutations and low CIN, indicating the essential role for MSH2 in MMR. On the other hand, a moderate DSBR defect is associated with the loss of either MSH2 or MSH3, whereas

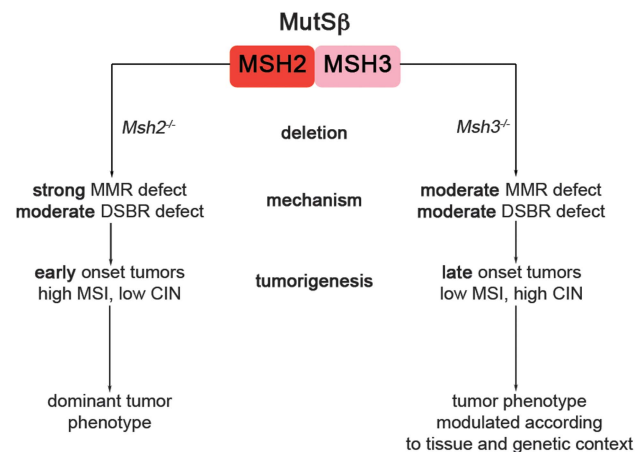


Figure 5. Model representing different functions of the MutSβ (MSH2-MSH3) complex. Deletion of *Msh2* induces a strong MMR defect and a moderate DSBR defect, leading to a dominant tumor phenotype with early-onset tumors that are MSI-high and chromosomally stable. Deletion of *Msh3* revealed a moderate DSBR defect next to the previously described moderate MMR defect, resulting in a modulated tumor phenotype of late-onset tumors that were MSI-low and showed increased CIN.

the mild phenotypes with regard to CIN and tumorigenesis that are associated with the loss of MSH2-MSH3-dependent DSBR are difficult to observe in the dominant MMR tumor phenotype of *Msh2*-deficient mice, we were able to study them by deleting *Msh3* on the appropriate tumor predisposing background. Because the DSBR defect is not as severe as the defect caused by loss of other canonical DSBR proteins, this further suggests a role for MSH3 in the repair of a subset of DSBs, possibly substrates of the SSA pathway.^{6,7} Interestingly, loss of MSH3 was shown to be associated with accelerated tumor progression in MLH1-deficient colorectal cancers, and it was suggested that the effect of MSH3 loss on tumor progression might be related to another function of MSH3 unrelated to MMR, implicating its role in DNA DSBR by SSA.³ It remains unclear whether the role of MSH3 in DSBR is dependent on its recruitment via the MMR pathway, either during the process of homologous recombination or when small insertions/deletions or DNA mismatches⁴³ on opposite strands are in close proximity so as to mediate the formation of DSBs during the MMR process, or whether MSH2-MSH3 could instead be recruited directly to sites of DSBs. Regardless, MSH3 was shown to co-localize with γH2AX and DSB foci following genotoxic stress,^{44,45} which suggests that it might be directly involved in a subset of DSBR events.

Despite the moderate defect in DSBR, *Msh3*-deficient mice showed a significant increase in sarcomagenesis, suggesting that loss of MSH3 targets sarcoma tumor suppressor genes and modulates *p53*-dependent tumorigenesis. When we analyzed lymphomas and sarcomas for genomic instability, *Msh3*^{−/−}*p53*^{−/−} and *p53*^{−/−} lymphomas showed the largest increase in CNV, whereas *Msh2*^{−/−}*p53*^{−/−} mice displayed a low CNV phenotype. Interestingly, both *Msh3/p53* and *p53* sarcomas displayed significantly more CNV than *Msh2/p53* lymphomas, but less CNV than *Msh3/p53* and *p53* lymphomas, and clustered together based on their moderate CNV profile. This indicates that loss of *Msh3* causes a repair defect that contributes to genomic instability in a tissue-specific manner and promotes *p53*-driven sarcomagenesis. As the sarcomas in our mouse cohorts are microsatellite stable, the increase in sarcoma incidence in *Msh3/p53* mutant mice is likely caused by loss of *Msh3*-dependent DSBR that contributes to the moderate CIN that is associated with sarcomagenesis. However, loss of *Msh3*-dependent MMR

might also have a role in *p53*-dependent sarcomagenesis by resulting in a low-level mutator phenotype involving base substitutions that might be difficult to detect.^{2,43}

In conclusion, our data indicate for the first time that the MSH2-MSH3 protein complex is involved in tumorigenesis through maintenance of chromosomal stability. In contrast to the MutS α complex (MSH2-MSH6), which has a dominant role in genome maintenance by MMR, MSH2-MSH3 functions both in MMR, indicated by an MSI-L phenotype, and DSB, as has been recently shown in yeast.⁷ Loss of MSH3 can therefore contribute to tumorigenesis in two ways: by a mild MMR defect leading to MSI-L and low-level mutation accumulation and by a DSB defect that leads to a moderate increase in CIN. As most sporadic colorectal cancers are CIN (85%),⁴⁶ the MSH2-MSH3 complex might have an important role in suppression of late-onset sporadic cancers that are MSI-L. Future studies should therefore include the analysis of *Msh3* loss on multiple tumorigenic backgrounds to assess a more specific role for MSH3 in tumorigenesis.

MATERIALS AND METHODS

Animals, tumors and survival

Msh2^{-/-}, *Msh3*^{-/-} and *Msh6*^{-/-} knockout mice were previously generated in our lab.^{13,28,47} *p53*^{-/-} knockout mice⁴⁸ were purchased from Jackson Laboratories (Bar Harbor, ME, USA). All mice were on a congenic C57BL/6 background. Mice were intercrossed as described and observed until they became morbid or moribund. Tumors were removed and fixed in 10% buffered formalin or frozen at -150 °C. After paraffin embedding of fixed tissue, sections were stained with hematoxylin and eosin. Statistical analysis of tumor incidence was completed using IBM SPSS Statistics version 20.0 (IBM Corp., Armonk, NY, USA). The Kaplan-Meier method was used to compare curves for survival, with significance evaluated by two-sided log rank statistics. A χ^2 -test was used to assess the influence of genotype on the tumor spectrum.

Microsatellite instability, LOH and mutational analysis of *p53*

For MSI analysis, the D7Mit91 and D17Mit123 microsatellite loci were amplified from normal and tumor DNA and analyzed as previously described.³⁹ Tumor DNA was also serially diluted and analyzed for loss of the wild-type *p53* allele as previously described.⁴² To analyze tumors for *p53* mutations, primers amplifying all exons of *p53* (including both transcript variants of exon 11) were used as described,⁴⁹ followed by DNA sequencing.

Chromatid break and double-strand break analysis

Primary MEFs (p4-6) were treated overnight with 0.1 μ g/ml colcemid (Invitrogen, Carlsbad, CA, USA) and subsequently swelled, fixed and dropped onto glass slides to prepare metaphase spreads. DNA was stained using mounting medium with DAPI (Vector Laboratories, Inc., Burlingame, CA, USA), and at least 100 metaphases in 2–3 different cell lines were analyzed per genotype.

For DSB analysis, MEFs were cultured on poly-L-lysine-coated slides (Sigma, St Louis, MO, USA), irradiated with 1 Gy and incubated at 37 °C for 30 min to 6 h. Cells were fixed with cold 1:1 methanol:acetone for 5 min, and washed twice with cold PBS for 5 min. After blocking with 10% FBS in PBS, cells were incubated overnight with a mouse monoclonal γ H2AX antibody (Upstate, Billerica, MA, USA; 1:500). Cells were again washed twice in cold PBS for 5 min and incubated for 1 h at room temperature with an Alexa Fluor 488-labeled goat anti-mouse antibody (Invitrogen). DNA was stained using mounting medium with DAPI. The experiment was repeated three times for two different cell lines per genotype, and a minimum of 100 cells were analyzed each time.

Metaphases and foci were counted using an Olympus BX61 microscope (Olympus America Inc., Center Valley, PA, USA) with Sensicam QE cooled CCD camera (PCO, Kelheim, Germany). Significant differences between cell lines in the number of breaks or γ H2AX foci were calculated using an independent two-sample *t*-test of equal variance.

Spectral karyotyping

Thymic lymphomas were dissociated, filtered and resuspended as described.⁵⁰ To prepare metaphase spreads, cells were treated with

colcemid for 3–6 h, swelled, fixed and dropped onto clean glass slides inside a humidity chamber. SKY was performed as previously described.⁵¹ Slides were hybridized with the combinatorially labeled whole chromosome painting probes (Applied Spectral Imaging, Inc., Carlsbad, CA, USA), and metaphase images were captured using the Applied Spectral Imaging interferometer on an epifluorescence microscope (Carl Zeiss Microscopy, Thornwood, NY, USA). SKY karyotypes were then analyzed with SkyView version 1.62 (Applied Spectral Imaging, Inc.). Metaphases were captured and analyzed using the nomenclature approved by the International Committee on Standardized Genetic Nomenclature for Mice (<http://www.informatics.jax.org>).

Array comparative genomic hybridization

Genomic DNA was isolated from frozen tumor tissue and matched normal tail tissue using the Qiagen DNeasy kit and hybridized to NimbleGen Mouse CGH 3 \times 720K Whole-Genome Tiling Arrays (Roche NimbleGen, Inc., Madison, WI, USA) in four different experiments. To represent the wide variation of mouse sarcoma samples but also to homogenize between genotypes, groups were composed of one fibrohistiocytic, one hemangio- and one spindle cell sarcoma each.

Plotting summaries of copy-number changes among all samples for each genotype was done as described before.⁴² In order to compare copy-number changes between different sets of samples, distributions of the (log2) ratios for the segmented data were plotted for each sample. The tails of this distribution (weight) were used to indicate the amount of CIN; that is, for each distribution, the proportion of data points >3 s.d. of the distribution with the lowest variance was computed on the left and right tails, that is, relative copy-number increase (gain) or decrease (loss) according to the aCGH data. Samples were subsequently clustered using the *k*-means clustering algorithm. Consistency of the clusters obtained was evaluated using the silhouette method.⁵²

CONFLICT OF INTEREST

The authors declare no conflict of interest.

ACKNOWLEDGEMENTS

We thank Rani Sellers from the Einstein Histotechnology and Comparative Pathology facility for mouse pathology and for reviewing the manuscript. This study was supported by National Institutes of Health grants CA76329 and CA93484 (WE), and CA72649 and CA102705 (MDS). MDS is supported by the Harry Eagle Chair provided by the National Women's Division of the Albert Einstein College of Medicine.

REFERENCES

- 1 Iyer RR, Pluciennik A, Burdett V, Modrich PL. DNA mismatch repair: functions and mechanisms. *Chem Rev* 2006; **106**: 302–323.
- 2 Marsischky GT, Kolodner RD. Biochemical characterization of the interaction between the *Saccharomyces cerevisiae* MSH2-MSH6 complex and mispaired bases in DNA. *J Biol Chem* 1999; **274**: 26668–26682.
- 3 Plaschke J, Kruger S, Jeske B, Theissig F, Kreuz FR, Pistorius S et al. Loss of MSH3 protein expression is frequent in MLH1-deficient colorectal cancer and is associated with disease progression. *Cancer Res* 2004; **64**: 864–870.
- 4 Evans E, Sugawara N, Haber JE, Alani E. The *Saccharomyces cerevisiae* Msh2 mismatch repair protein localizes to recombination intermediates *in vivo*. *Mol cell* 2000; **5**: 789–799.
- 5 Sugawara N, Paques F, Colaiacovo M, Haber JE. Role of *Saccharomyces cerevisiae* Msh2 and Msh3 repair proteins in double-strand break-induced recombination. *Proc Natl Acad Sci USA* 1997; **94**: 9214–9219.
- 6 Lyndaker AM, Alani E. A tale of tails: insights into the coordination of 3' end processing during homologous recombination. *Bioessays* 2009; **31**: 315–321.
- 7 Kumar C, Williams GM, Havens B, Dinicola M, Surtees JA. Distinct requirements within the Msh3 nucleotide binding pocket for mismatch and double-strand break repair. *J Mol Biol* 2013; **425**: 1881–1898.
- 8 Manley K, Shirley TL, Flaherty L, Messer A. Msh2 deficiency prevents *in vivo* somatic instability of the CAG repeat in Huntington disease transgenic mice. *Nature Genet* 1999; **23**: 471–473.
- 9 Owen BA, Yang Z, Lai M, Gajec M, Badger 2nd JD, Hayes JJ et al. (CAG)(n)-hairpin DNA binds to Msh2-Msh3 and changes properties of mismatch recognition. *Nat Struct Mol Biol* 2005; **12**: 663–670.

- 10 Savouret C, Brisson E, Essers J, Kanaar R, Pastink A, te Riele H *et al*. CTG repeat instability and size variation timing in DNA repair-deficient mice. *EMBO J* 2003; **22**: 2264–2273.
- 11 van den Broek WJ, Nelen MR, Wansink DG, Coerwinkel MM, te Riele H, Groenen PJ *et al*. Somatic expansion behaviour of the (CTG)_n repeat in myotonic dystrophy knock-in mice is differentially affected by Msh3 and Msh6 mismatch-repair proteins. *Hum Mol Genet* 2002; **11**: 191–198.
- 12 Tome S, Holt I, Edelmann W, Morris GE, Munnich A, Pearson CE *et al*. MSH2 ATPase domain mutation affects CTG/CAG repeat instability in transgenic mice. *PLoS Genet* 2009; **5**: e1000482.
- 13 Edelmann W, Umar A, Yang K, Heyer J, Kucherlapati M, Lia M *et al*. The DNA mismatch repair genes Msh3 and Msh6 cooperate in intestinal tumor suppression. *Cancer Res* 2000; **60**: 803–807.
- 14 Plaschke J, Preussler M, Ziegler A, Schackert HK. Aberrant protein expression and frequent allelic loss of MSH3 in colorectal cancer with low-level microsatellite instability. *Int J Colorectal Dis* 2012; **27**: 911–919.
- 15 Haugen AC, Goel A, Yamada K, Marra G, Nguyen TP, Nagasaka T *et al*. Genetic instability caused by loss of MutS homologue 3 in human colorectal cancer. *Cancer Res* 2008; **68**: 8465–8472.
- 16 Lee SY, Chung H, Devaraj B, Iwazumi M, Han HS, Hwang DY *et al*. Microsatellite alterations at selected tetranucleotide repeats are associated with morphologies of colorectal neoplasias. *Gastroenterol* 2010; **139**: 1519–1525.
- 17 Benachenhou N, Guiral S, Gorska-Flipot I, Labuda D, Sinnett D. High resolution deletion mapping reveals frequent allelic losses at the DNA mismatch repair loci hMLH1 and hMSH3 in non-small cell lung cancer. *Int J Cancer* 1998; **77**: 173–180.
- 18 Kawakami T, Shiina H, Igawa M, Deguchi M, Nakajima K, Ogishima T *et al*. Inactivation of the hMSH3 mismatch repair gene in bladder cancer. *Biochem Biophys Res Comm* 2004; **325**: 934–942.
- 19 Benachenhou N, Guiral S, Gorska-Flipot I, Labuda D, Sinnett D. Frequent loss of heterozygosity at the DNA mismatch-repair loci hMLH1 and hMSH3 in sporadic breast cancer. *Br J Cancer* 1999; **79**: 1012–1017.
- 20 Berndt SI, Platz EA, Fallin MD, Thuita LW, Hoffman SC, Helzlsouer KJ. Mismatch repair polymorphisms and the risk of colorectal cancer. *Int J cancer* 2007; **120**: 1548–1554.
- 21 Orimo H, Nakajima E, Yamamoto M, Ikejima M, Emi M, Shimada T. Association between single nucleotide polymorphisms in the hMSH3 gene and sporadic colon cancer with microsatellite instability. *J Hum Genet* 2000; **45**: 228–230.
- 22 Hirata H, Hinoda Y, Kawamoto K, Kikuno N, Suehiro Y, Okayama N *et al*. Mismatch repair gene MSH3 polymorphism is associated with the risk of sporadic prostate cancer. *J Urol* 2008; **179**: 2020–2024.
- 23 Michiels S, Danoy P, Dessen P, Bera A, Boulet T, Bouchardy C *et al*. Polymorphism discovery in 62 DNA repair genes and haplotype associations with risks for lung and head and neck cancers. *Carcinogenesis* 2007; **28**: 1731–1739.
- 24 Tome S, Simard JP, Slean MM, Holt I, Morris GE, Wojciechowski K *et al*. Tissue-specific mismatch repair protein expression: MSH3 is higher than MSH6 in multiple mouse tissues. *DNA repair* 2013; **12**: 46–52.
- 25 Cranston A, Bocker T, Reitmaier A, Palazzo J, Wilson T, Mak T *et al*. Female embryonic lethality in mice nullizygous for both Msh2 and p53. *Nature Genet* 1997; **17**: 114–118.
- 26 Reitmaier AH, Schmits R, Ewel A, Bapat B, Redston M, Mitri A *et al*. MSH2 deficient mice are viable and susceptible to lymphoid tumours. *Nature Genet* 1995; **11**: 64–70.
- 27 de Wind N, Dekker M, Berns A, Radman M, te Riele H. Inactivation of the mouse Msh2 gene results in mismatch repair deficiency, methylation tolerance, hyper-recombination, and predisposition to cancer. *Cell* 1995; **82**: 321–330.
- 28 Smits R, Hofland N, Edelmann W, Geugien M, Jagmohan-Changur S, Albuquerque C *et al*. Somatic Apc mutations are selected upon their capacity to inactivate the beta-catenin downregulating activity. *Genes Chromosomes Cancer* 2000; **29**: 229–239.
- 29 Toft NJ, Curtis LJ, Sansom OJ, Leitch AL, Wyllie AH, te Riele H *et al*. Heterozygosity for p53 promotes microsatellite instability and tumorigenesis on a Msh2 deficient background. *Oncogene* 2002; **21**: 6299–6306.
- 30 Jacks T. Lessons from the p53 mutant mouse. *J Cancer Res Clin Oncol* 1996; **122**: 319–327.
- 31 Miura T, Yamana Y, Usui T, Ogawa HI, Yamamoto MT, Kusano K. Homologous recombination via synthesis-dependent strand annealing in yeast requires the Irc20 and Srs2 DNA helicases. *Genetics* 2012; **191**: 65–78.
- 32 Chen PC, Dudley S, Hagen W, Dizon D, Paxton L, Reichow D *et al*. Contributions by MutL homologues Mlh3 and Pms2 to DNA mismatch repair and tumor suppression in the mouse. *Cancer Res* 2005; **65**: 8662–8670.
- 33 Bardwell PD, Woo CJ, Wei K, Li Z, Martin A, Sack SZ *et al*. Altered somatic hypermutation and reduced class-switch recombination in exonuclease 1-mutant mice. *Nat Immunol* 2004; **5**: 224–229.
- 34 Li Z, Peled JU, Zhao C, Svetlanov A, Ronai D, Cohen PE *et al*. A role for Mlh3 in somatic hypermutation. *DNA Repair* 2006; **5**: 675–682.
- 35 Li Z, Scherer SJ, Ronai D, Iglesias-Ussel MD, Peled JU, Bardwell PD *et al*. Examination of Msh6- and Msh3-deficient mice in class switching reveals overlapping and distinct roles of MutS homologues in antibody diversification. *J Exp Med* 2004; **200**: 47–59.
- 36 Wu X, Tsai CY, Patam MB, Zan H, Chen JP, Lipkin SM *et al*. A role for the MutL mismatch repair Mlh3 protein in immunoglobulin class switch DNA recombination and somatic hypermutation. *J Immunol* 2006; **176**: 5426–5437.
- 37 Svetlanov A, Baudat F, Cohen PE, de Massy B. Distinct functions of MLH3 at recombination hot spots in the mouse. *Genetics* 2008; **178**: 1937–1945.
- 38 Tomimatsu N, Mukherjee B, Deland K, Kurimasa A, Bolderson E, Khanna KK *et al*. Exo1 plays a major role in DNA end resection in humans and influences double-strand break repair and damage signaling decisions. *DNA Repair* 2012; **11**: 441–448.
- 39 Kuraguchi M, Yang K, Wong E, Advievich E, Fan K, Kolodner RD *et al*. The distinct spectra of tumor-associated Apc mutations in mismatch repair-deficient Apc1638N mice define the roles of MSH3 and MSH6 in DNA repair and intestinal tumorigenesis. *Cancer Res* 2001; **61**: 7934–7942.
- 40 Fukasawa K, Choi T, Kuriyama R, Rulong S, Vande Woude GF. Abnormal centrosome amplification in the absence of p53. *Science* 1996; **271**: 1744–1747.
- 41 Tomasini R, Mak TW, Melino G. The impact of p53 and p73 on aneuploidy and cancer. *Trends Cell Biol* 2008; **18**: 244–252.
- 42 Wang Y, Zhang W, Edelmann L, Kolodner RD, Kucherlapati R, Edelmann W. Cis lethal genetic interactions attenuate and alter p53 tumorigenesis. *Proc Natl Acad Sci USA* 2010; **107**: 5511–5515.
- 43 Harrington JM, Kolodner RD. *Saccharomyces cerevisiae* Msh2-Msh3 acts in repair of base-base mismatches. *Mol Cell Biol* 2007; **27**: 6546–6554.
- 44 Hong Z, Jiang J, Hashiguchi K, Hoshi M, Lan L, Yasui A. Recruitment of mismatch repair proteins to the site of DNA damage in human cells. *J Cell Sci* 2008; **121** (Pt 19): 3146–3154.
- 45 Reynolds MF, Peterson-Roth EC, Bernalov IA, Johnston T, Gurel VM, Menard HL *et al*. Rapid DNA double-strand breaks resulting from processing of Cr-DNA cross-links by both MutS dimers. *Cancer Res* 2009; **69**: 1071–1079.
- 46 Pino MS, Chung DC. The chromosomal instability pathway in colon cancer. *Gastroenterology* 2010; **138**: 2059–2072.
- 47 Edelmann W, Yang K, Umar A, Heyer J, Lau K, Fan K *et al*. Mutation in the mismatch repair gene Msh6 causes cancer susceptibility. *Cell* 1997; **91**: 467–477.
- 48 Jacks T, Remington L, Williams BO, Schmitt EM, Halachmi S, Bronson RT *et al*. Tumor spectrum analysis in p53-mutant mice. *Curr Biol* 1994; **4**: 1–7.
- 49 Varela I, Klijn C, Stephens PJ, Mudie LJ, Stebbings L, Galappaththige D *et al*. Somatic structural rearrangements in genetically engineered mouse mammary tumors. *Genome Biol* 2010; **11**: R100.
- 50 Peled JU, Sellers RS, Iglesias-Ussel MD, Shin DM, Montagna C, Zhao C *et al*. Msh6 protects mature B cells from lymphoma by preserving genomic stability. *Am J Pathol* 2010; **175**: 2597–2608.
- 51 Schrock E, du Manoir S, Veldman T, Schoell B, Wienberg J, Ferguson-Smith MA *et al*. Multicolor spectral karyotyping of human chromosomes. *Science* 1996; **273**: 494–497.
- 52 Rousseeuw PJ. Silhouettes: A graphical aid to the interpretation and validation of cluster analysis. *J Comput Appl Math* 1987; **20**: 53–65.

Supplementary Information accompanies this paper on the Oncogene website (<http://www.nature.com/onc>)